Shock and Vibration 18 (2011) 13–27
DOI 10.3233/SAV-2010-0588
IOS Press

Analysis of dynamic characteristics for a rotor system with pedestal looseness

Hui Ma*, Xueyan Zhao, Yunnan Teng and Bangchun Wen
School of Mechanical Engineering and Automation, Northeastern University, Shenyang, Liaoning 110819, P.R. China

Received 9 February 2010
Revised 10 May 2010

Abstract. This paper presents a finite element model of a rotor system with pedestal looseness stemming from a loosened bolt and analyzes the effects of the looseness parameters on its dynamic characteristics. When the displacement of the pedestal is less than or equal to the looseness clearance, the motion of the rotor varies from period-one through period-two and period-three to period-five with the decreasing of stiffness of the non-loosened bolts. The similar bifurcation phenomenon can be also observed during the increasing process of the rotational speed. But the rotor motion is from period-six through period-three to period-four with the decreasing of the foundation stiffness. When the stiffness of the foundation is small and the displacement of pedestal is greater than the looseness clearance, the response of the rotor exhibits period-one and high order harmonic components with the decreasing of looseness clearance, such as 2X, 3X etc. However, when the stiffness of the foundation is great, the spectrum of the response of the rotor will be from combined frequency components to the continuous spectrum with the decreasing of the looseness clearance.

Keywords: Nonlinear Vibration, rotor system, pedestal looseness, finite element method

Nomenclature

a	Distance between coupling gravity center and left bearing
c_{bl}	Foundation equivalent damping
c_{xl}, c_{yl}	Horizontal (vertical) damping of left bearing
d_1, d_2	Journal diameter and shaft diameter at the impeller
E	Elastic modulus
k_b	Foundation stiffness
k_{b1}	Stiffness of non-loosened bolts
k_{b2}	Stiffness of loosened bolts
k_{bl}	Left pedestal equivalent stiffness
k_{xl}, k_{yl}	Horizontal (vertical) stiffness of left bearing
l	Center distance between left bearing and right bearing
l_1	Distance between impeller gravity center and left bearing
$m \cdot r$	Unbalance moment
m_1	coupling mass
m_2	Impeller mass
m_{bl}	Left pedestal mass
$O_i (i = 1, 2, 3, 4)$	Geometric center

*Corresponding author: Hui Ma, Tel.: +86 24 83671429; Fax: +86 24 83679731; E-mail: mahui_2007@163.com.

ISSN 1070-9622/11/$27.50

O_{m2}	Impeller centroid
y_b	Pedestal displacement
δ_1	Looseness clearance
υ	Poisson ratio
ρ	Material density
ω	Rotational speed (rev/min)

1. Introduction

In a rotor-bearing system, the loosened bolt of the pedestal will reduce pedestal stiffness, mechanical damping, which results in violent vibration of the whole system. Especially, when the looseness fault is serious, it may cause other faults such as rub-impact fault of the rotor-stator, even may lead to disastrous accidents [1,2]. Therefore, the research on pedestal looseness is significant in engineering practice for the safe operation of rotating machinery, the extension of service life, the improvement of its work efficiency.

In the last decades, dynamics and fault diagnosis of rotor systems with pedestal looseness have attracted the attention of many researchers and many results were obtained. Goldman and Muszynska [3] proposed the bi-linear model of a rotating machine with one loose pedestal. Their numeric results showed the synchronous and subsynchronous fractional components of the response, which were verified by the experiments. Subsequently, they discussed the chaotic behavior of the system based on the bi-linear model [4]. Chu and Tang [5] analyzed vibration characteristics of a rotor-bearing system with pedestal looseness by building a non-linear mathematical model. Stability of these periodic solutions was discussed by using the shooting method and the Floquet theory. When the rotational speed and imbalance of rotors varied, periodic, quasi-periodic and chaotic motions could be observed and three kinds of routes to or out of chaos were found. In some cases, pedestal looseness could results in 1X/2 fractional harmonic and multiple harmonic motions of rotor-bearing systems [6]. Using the nonlinear bearing pedestal model composed of a non-linear spring and a linear damping, Ji [7] analyzed the free and forced vibration of a non-linear bearing system to illustrate the non-linear effect on the free and forced vibrations of the system by the method of multiple scales. Ma [8] set up a mechanical model of looseness of fastening bolt on the bearing pedestal and investigated the dynamic characteristics of rotor by using the nonlinear oil-film model put forward by Adiletta. The results show that system motion state changes frequently with the increase of the rotational speed. Fault diagnosis of rotor systems with pedestal looseness have been performed using different analytical methods, such as genetic algorithm, Hilbert-Huang Transform and wavelet packets-fractal technology [9–11].

Recently, many researchers studied rotor fault by using finite element method which may take into account many factors, such as mass, moment inertia, internal damping, bending and torsion vibration coupling effects. Chien [12] presented the dynamic responses of the coupled textile/rotor system by finite element analysis. The effects of constant and non-constant angular rotational speeds, shaft stiffness and non-linear terms on the transient amplitudes of the textile and the whirling deflection of the shaft are investigated. Jing [13] studied the nonlinear dynamic behavior of a rotor-bearing system based on a continuum model using the finite element method in his analysis. By comparing with a simple discrete model, some significant difference is found between two models. By combining finite element model of rotor and rigid discs, Han [14] presented a quantitative identification procedure for local rubbing fault in rotor systems based on a hybrid model and identified oil film stiffness and elastic supports. Guo [15] built the rotor model with a growth crack by finite element method (FEM) and Dimarogonas' method, investigated crack fault using HHT. For shaft crack detection, a genetic algorithm [16] was proposed, which can make the shaft crack detection as an optimization problem by means of the finite element method. Behzad [17] developed a finite-element code for studying the effects of loose rotating discs on the rotor–bearing systems' response. The developed finite-element model can numerically give the response of rotors with any number of loose discs at any location with isotropic or orthotropic supports. Considering a base-transferred shock force, Lee [18] presented a generalized finite element modeling method of a rotor-bearing system using the state-space Newmark method based on the average velocity concept.

Most of previous researches on looseness fault focus on simple Jeffcott rotor systems using the lumped mass model and only a few works were on the complex rotor system with looseness fault using finite element method

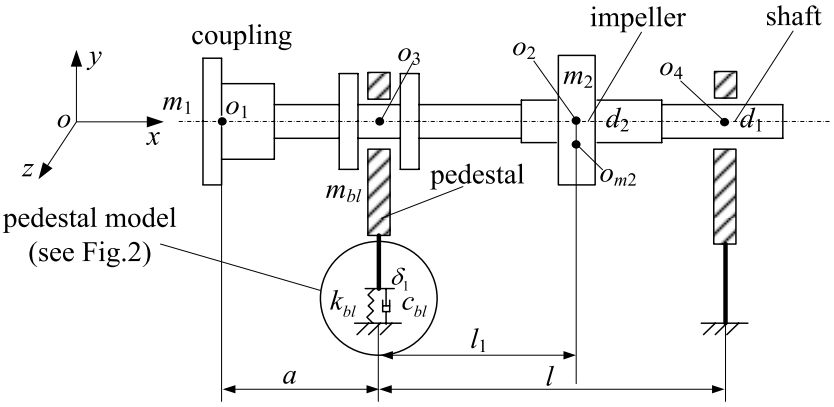

Fig. 1. Mechanical model of the rotor-bearing-foundation system.

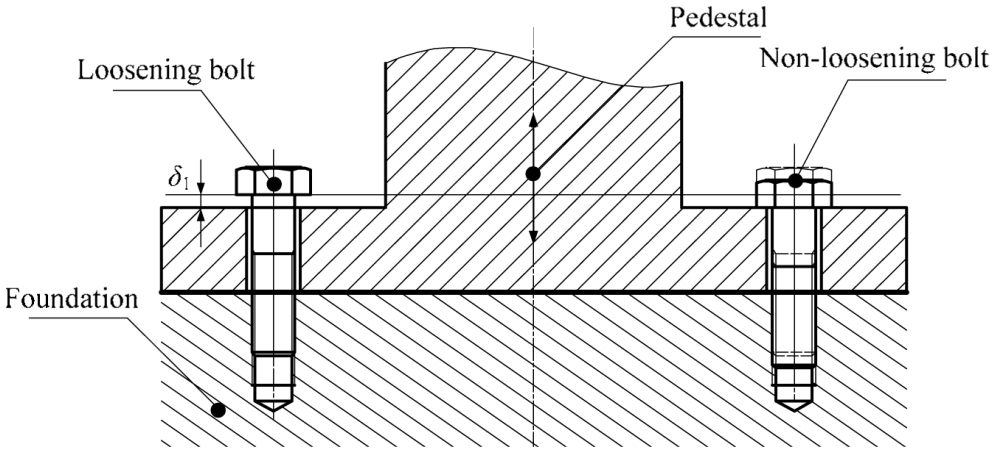

Fig. 2. Bolt looseness schematic.

(FEM). In our study, a nonlinear finite element model of the rotor-bearing-foundation system with pedestal looseness is set up. Vibration responses are simulated by changing different looseness parameters. When the displacement of pedestal is less than or equal to looseness clearance and some influence parameters such as stiffness of non-loosened bolts, rotational speed, and foundation stiffness are considered. When the displacement of pedestal is greater than looseness clearance, the responses are simulated under different foundation stiffnesses. The results may give deep insight into looseness mechanism.

This paper investigates the dynamic characteristics of a rotor system with pedestal looseness. The next of the paper is organized as follows: The mathematical model of the considered system is described in Section 2. In Section 3, dynamic characteristics of rotor system with pedestal looseness when $y_b \leqslant \delta_1$ is studied, the effect of stiffness of non-loosened bolts is analyzed in Section 3.1, the effect of rotational speed in Section 3.2, and the effect of foundation stiffness in Section 3.3. In Section 4, vibration characteristics of rotor system with pedestal looseness when $y_b > \delta_1$ are analyzed, the effect of looseness clearance under small foundation stiffness condition is analyzed in Section 4.1, and the effect for looseness clearance under large foundation stiffness condition is analyzed in Section 4.2. Conclusions are given in Section 5.

2. Mathematical models of a rotor system with pedestal looseness

Figure 1 shows the mechanical model of the considered rotor system, which consists of two identical tilting-pad bearings, a coupling, an impeller and a stepped shaft. Each tilting-pad bearing is supported on one pedestal, which

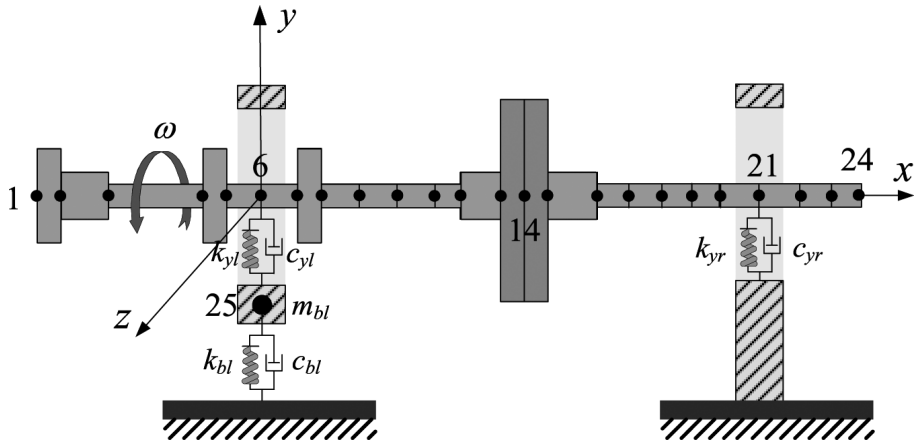

Fig. 3. The finite element model of the rotor-bearing-foundation system.

is fixed on the foundation by two bolts. It is assumed that one bolt on the left pedestal is loosened, which causes the pedestal loose, as is shown in Fig. 2. In the following context, the equivalent stiffness of pedestal will be described by bi-linear and tri-linear forms.

In this paper, the equivalent stiffness of pedestal can be simplified as

$$k_{bl} \approx \begin{cases} k_{b1}\ 0 \leqslant y_b \leqslant \delta_1 \\ k_b,\ others \end{cases} . \tag{1}$$

Considering the directivity of looseness fault, in this paper, only the vibration characteristics of the rotor system with looseness fault in vertical direction y are studied. And assume that pedestal equivalent damping (c_{bl}) is constant.

2.1. Finite element model of rotor system with looseness fault

The finite element model of rotor-bearing-foundation is established, only the stiffness and the damping of bearing and pedestal are plotted in vertical direction, as is shown in Fig. 3. In the figure, black spots denote nodes, number denotes node number, impeller and coupling are simplified as discs, left and right tilting pad bearings are simulated by four oil film stiffness coefficients and four oil film damping coefficients. The equivalent stiffness of loosening pedestal can be obtained by Eq. (1).

The dynamic equation of the rotor system with looseness fault by finite element method is shown as follows:

$$\boldsymbol{M\ddot{q}} + \boldsymbol{D\dot{q}} + \boldsymbol{Kq} = \boldsymbol{Q} \tag{2}$$

Where $\boldsymbol{M}$ is mass matrix including shaft, disc and pedestal, $\boldsymbol{D}$ is damping matrix including bearing damping, gyroscopic matrix and foundation equivalent damping, $\boldsymbol{K}$ is global stiffness matrix, $\boldsymbol{Q}$ is composite external force vector, $\boldsymbol{q}$ is displacement vector. Finally, Eq. (2) is solved by using the Newmark-β method to obtain the displacement of rotor.

3. Dynamic characteristics of the rotor system with pedestal looseness when $y_b \leqslant \delta_1$

Values for the parameters of the rotor system used in the analysis and the subsequent simulation are as follows: $d_1 = 40$ mm, $d_2 = 51$ mm, $l = 0.8$ m, $a = 0.208$ m, $l_1 = 0.54$ m, $E = 2.07 \times 10^{11}$ Pa, $\upsilon = 0.3$, $\rho = 7850$ kg/m^3, $k_{xl} = 2.2 \times 10^8$ N/m, $k_{yl} = 3.6 \times 10^8$ N/m, $c_{xl} = 6.43 \times 10^5$ N·s/m, $c_{yl} = 8.8 \times 10^5$ N·s/m, $c_{bl} = 2 \times 10^5$ N·s/m, $\delta_1 = 1$ mm, $m_{bl} = 32$ kg, $m \cdot r = 168.5$ g·mm. The bearing parameters of right end are identical as these of left end. Based on these values the first critical speed of the rotor system is obtained as 4135 rev/min.

For the normal rotor systems, the amplitudes (peak-peak value) of different nodes at different rotating speeds(2000, 4000 and 6000 rev/min), are simulated by taking $k_b = k_{b1} = 4 \times 10^7$ N/m, as is shown in Fig. 4. From this

Table 1
Simulation conditions when $y_b \leqslant \delta_1$

Fixed-parameter	Variable parameters	Figures
$k_{b1} = 4 \times 10^7$ N/m, $k_b = 4 \times 10^7$ N/m, $\delta_1 = 1$ mm	ω	Fig. 4
$\omega = 4000$ rev/min, $k_b = 4 \times 10^7$ N/m, $\delta_1 = 1$ mm	k_{b1}	Fig. 5, Fig. 6
$k_b = 4 \times 10^7$ N/m, $k_{b1} = 2.2 \times 10^5$ N/m, $\delta_1 = 1$ mm	ω	Fig. 7
$\omega = 4000$ rev/min, $k_{b1} = 2.2 \times 10^5$N/m, $\delta_1 = 1$ mm	k_b	Fig. 8

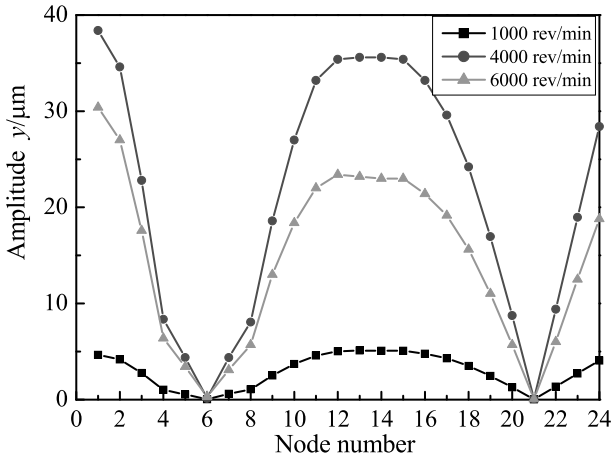

Fig. 4. Amplitudes under different rotating speeds.

figure, it can be seen that the amplitude of journal in left bearing (node 6) is closed to zero at given three rotating speeds. In the following we investigate the dynamic characteristics of rotor system with pedestal looseness when $y_b \leqslant \delta_1$. The pedestal equivalent stiffness is given by Eq. (1). The effect of different parameters on the dynamic characteristics of the rotor system is studied. These parameters include stiffness of non-loosened bolts, rotational speed and foundation stiffness. The simulation conditions are listed in Table 1. The figures (Figs 5–10), from the top to the bottom, are vibration waveform, amplitude spectrum and rotor trajectory, respectively.

3.1. The effect of stiffness of non-loosened bolts (k_{b1})

Pedestal is likely to become loose when rotational speed is approaching to the first critical speed (4135 rev/min). Therefore, we choose the simulation condition as $\omega = 6000$ rev/min (around the first critical speed), $k_b = 4 \times 10^7$ N/m, and $\delta_1 = 1$ mm (much larger than y_b).

It can be seen from Fig. 5(a) that when $k_{b1}/k_b = 0.05$, vibration amplitude is 6.1 μm. The waveform is a sine-cosine curve and the average displacement is much greater than zero due to piecewise linear stiffness. In the frequency domain, high order frequency components (i.e. 2X, 3X, 4X, etc.) can be observed but their amplitudes decrease along with the increase of the frequency. In such case, the rotor motion is period-one. Rotor trajectory is a long and narrow ellipse along the direction of arrows. This is because horizontal stiffness (z-coordinate) is far greater than vertical stiffness (y-coordinate).

Figure 5(b) displays vibration characteristics of node 6 when $k_{b1}/k_b = 0.025$. In time domain, vibration amplitude increases and is about 9.3 μm. The period of motion is two times as long as that of the former, which also show the amount of beating is 1/2 times of that in Fig. 5(a). Obviously the waveform is truncated near wave troughs. This is due to periodic beating when the pedestal contacts foundation instantly. In frequency domain, the amplitude spectrum shows 1/2 fractional harmonic components (i.e. 1X/2, 3X/2, 4X/2, etc.), which indicates that the rotor reaches a period-two motion, and the amplitude of 1X/2 component is greater than the others. Furthermore, the rotor trajectory displays the shape of '8' curve and its motion direction is also shown by arrows. In such case, it is clear that bifurcation phenomenon appears when the stiffness of non-loosened bolts decreases.

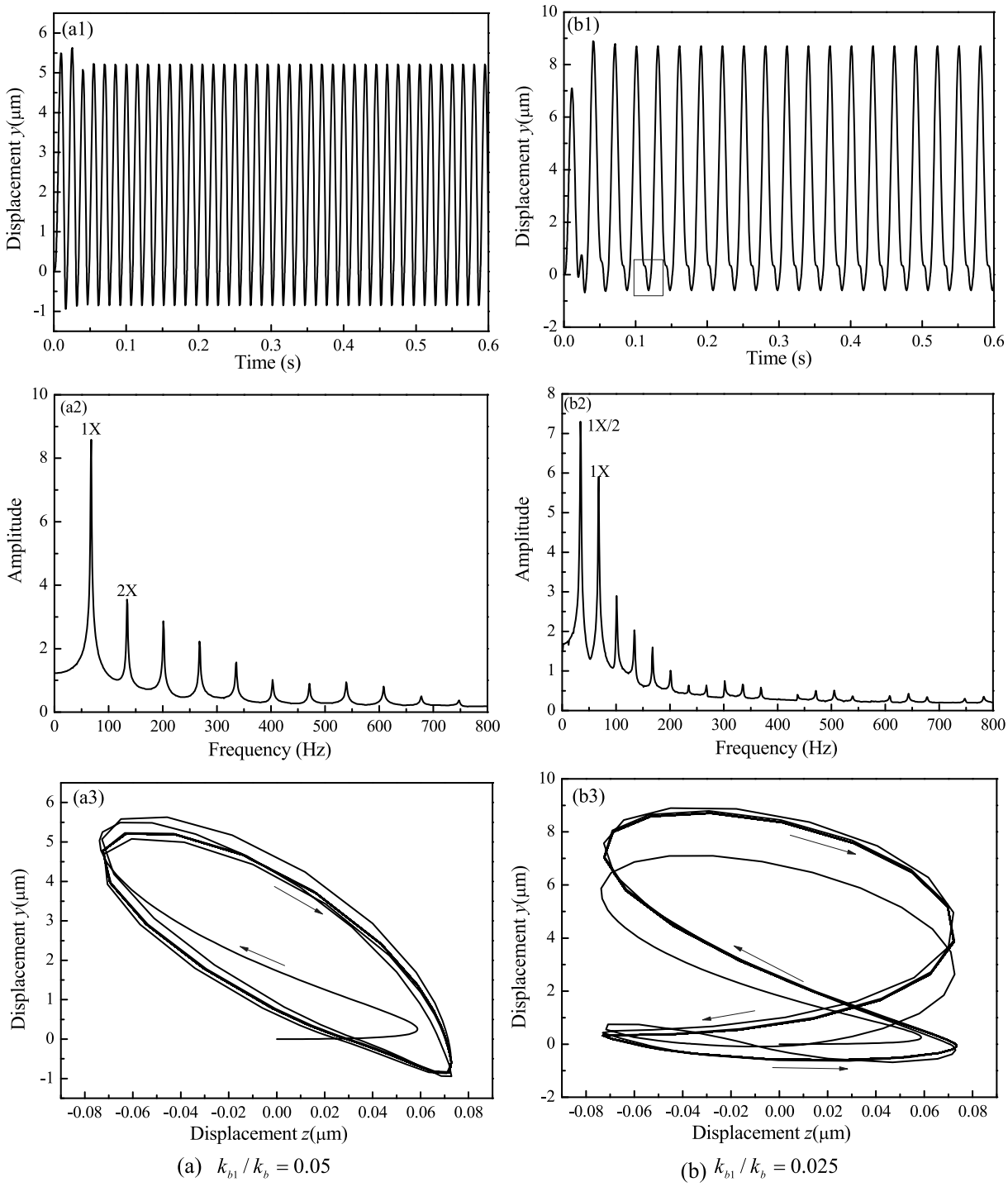

Fig. 5. Vibration characteristics of node 6 when $k_{b1}/k_b = 0.05$ and $k_{b1}/k_b = 0.025$.

The system motion form changes to period-three when the stiffness of non-loosened bolts continues declining ($k_{b1}/k_b = 0.0055$), as is shown in Fig. 6(a). The vibration amplitude is almost unchanged compared with that in Fig. 5(b). But the 1/3 fractional harmonic components (i.e. 1X/3, 2X/3, and 4X/3, etc.) can be observed from the

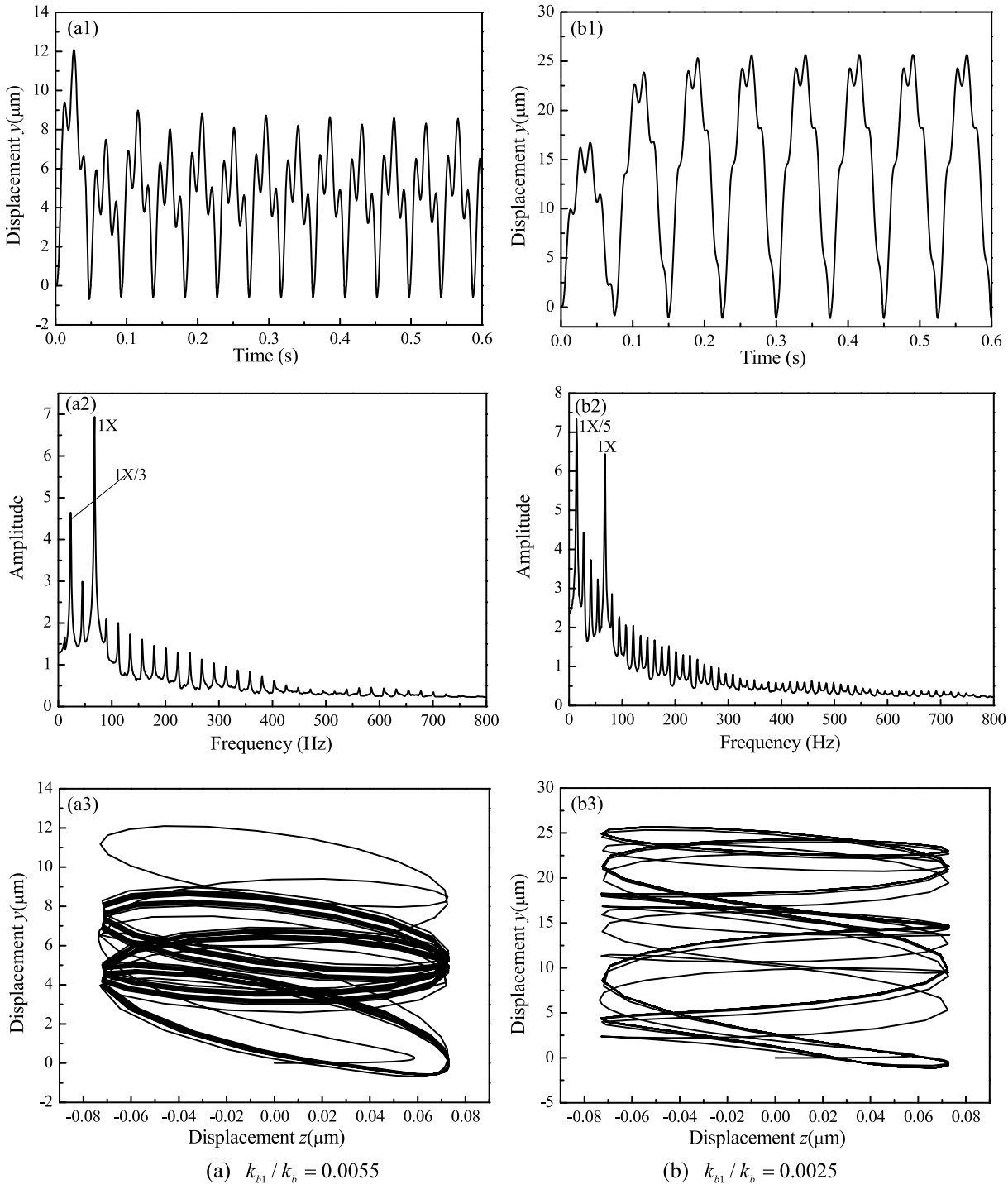

Fig. 6. Vibration characteristics of nodes 6 when $k_{b1}/k_b = 0.0055$ and $k_{b1}/k_b = 0.0025$.

amplitude spectrum and the amplitude of 1X/3 is second only to that of 1X component. Rotor trajectory looks like the shape of multiple inside '8' curve.

Figure 6 (b) demonstrates the system responses when $k_{b1}/k_b = 0.0025$. Noticeably, vibration period becomes

Table 2
Vibration characteristics of pedestal looseness with decrease of k_{b1}

Fixed-parameter	k_{b1}/k_b	Amplitude (peak-peak value μm)	Frequency spectrum characteristics	Motion forms	Rotor trajectory characteristics
$\omega = 4000$ rev/min	0.05	6.1	High order frequency components (1X, 2X, 3X, etc.)	Period-one (P-1)	A long and narrow elliptic
$\delta_1 = 1$ mm	0.025	9.3	The 1/2 fractional harmonic components (1X/2,1X,3X/2,etc.)	P-2	"8" shape curve
$k_b = 4 \times 10^7$ N/m	0.0055	9.4	The 1/3 fractional harmonic components	P-3	Multiple inside '8' curve
	0.0025	26.8	The 1/5 fractional harmonic components	P-5	Spiral curve

Table 3
Response features of pedestal looseness with increase of ω

Fixed-parameter	ω (rev/min)	Amplitude (peak-peak value μm)	Frequency spectrum characteristics	Motion forms	Rotor trajectory characteristics
$\delta_1 = 1$ mm	2000	8.2	The 1/2 fractional harmonic components (1X/2, 1X, 3X/2, etc.)	P-2	"8" shape curve
$k_{b1} = 2.2 \times 10^5$ N/m	4000	9.4	The 1/3 fractional harmonic components	P-3	Multiple inside '8' curve
$k_b = 4 \times 10^7$ N/m	6000	20	The 1/5 fractional harmonic components	P-5	Spiral curve

longer and the vibration amplitude reaches at the value of 26.8 μm. In frequency domain, the 1/5 fractional harmonic components (i.e. 1X/5, 2X/5, etc.) can be observed and the amplitude of 1X/5 component is largest. In such case, system motion is period-five. Rotor trajectory likes as spiral along with vertical direction. All these characteristics indicate that the looseness is very serious.

The detailed Vibration characteristics of pedestal looseness with the decrease of k_{b1} are listed in Table 2. When the pedestal stiffness becomes smaller, vibration amplitude increases gradually, even reach at 26.8 μm which exceeds allowable amplitude of 15 μm. Low frequency components with large amplitude can be observed in frequency spectrum. Rotor trajectory changes from a long and narrow elliptic to a spiral curve. By above analysis, we can conclude that when looseness becomes more and more serious, system motion demonstrates bifurcation characteristics and the amplitude of minimum frequency component is maximum or second.

3.2. The effect of rotational speed

Rotational speed is an important parameter affecting the vibration of the rotor system. Figure 7 shows the vibration of node 6 with different rotational speeds $\omega = 2000$ rev/min (less than first critical speed) and $\omega = 6000$ rev/min (greater than first critical speed) respectively, when $k_{b1} = 2 \times 10^5$ N/m, $k_b = 4 \times 10^7$ N/m and $\delta_1 = 1$ mm.

It can be seen from Fig. 7(a) that when $\omega = 2000$ rev/min, vibration amplitude is about 8 μm and the waveform is truncated near wave trough. In frequency domain, the 1/2 fractional harmonic components such as 1X/2 and 3X/2, etc. can be observed, which shows that system motion is period-two and the amplitude of 1X/2 is the largest. Rotor trajectory displays the shape of '8' curve. Compared with Fig. 5 (b), the waveform, amplitude spectrum and trajectory in Fig. 7 (a) are similar to these in Fig. 5(b).

Figure 7(b) displays that when $\omega = 6000$ rev/min, vibration is aggravated with the amplitude of 20 μm because of the increase of rotational speed. In frequency domain, the amplitude spectrum shows the 1/5 fractional harmonic components such as 1X/5 and 2X/5, etc. can be observed, which shows system motion is period-five and the amplitude of 1X/5 is second only to that of 1X. Rotor trajectory likes as a spiral along with vertical direction. All this vibration characteristics are similar to these shown in Fig. 6(b).

The detailed response features of pedestal looseness with increase of ω are listed in Table 3. By Comparing Table 2 with Table 3, we can conclude that the decrease of stiffness of non-loosened bolts has the similar effect on the vibration of node 6 to increase of rotational speed (unbalance force).

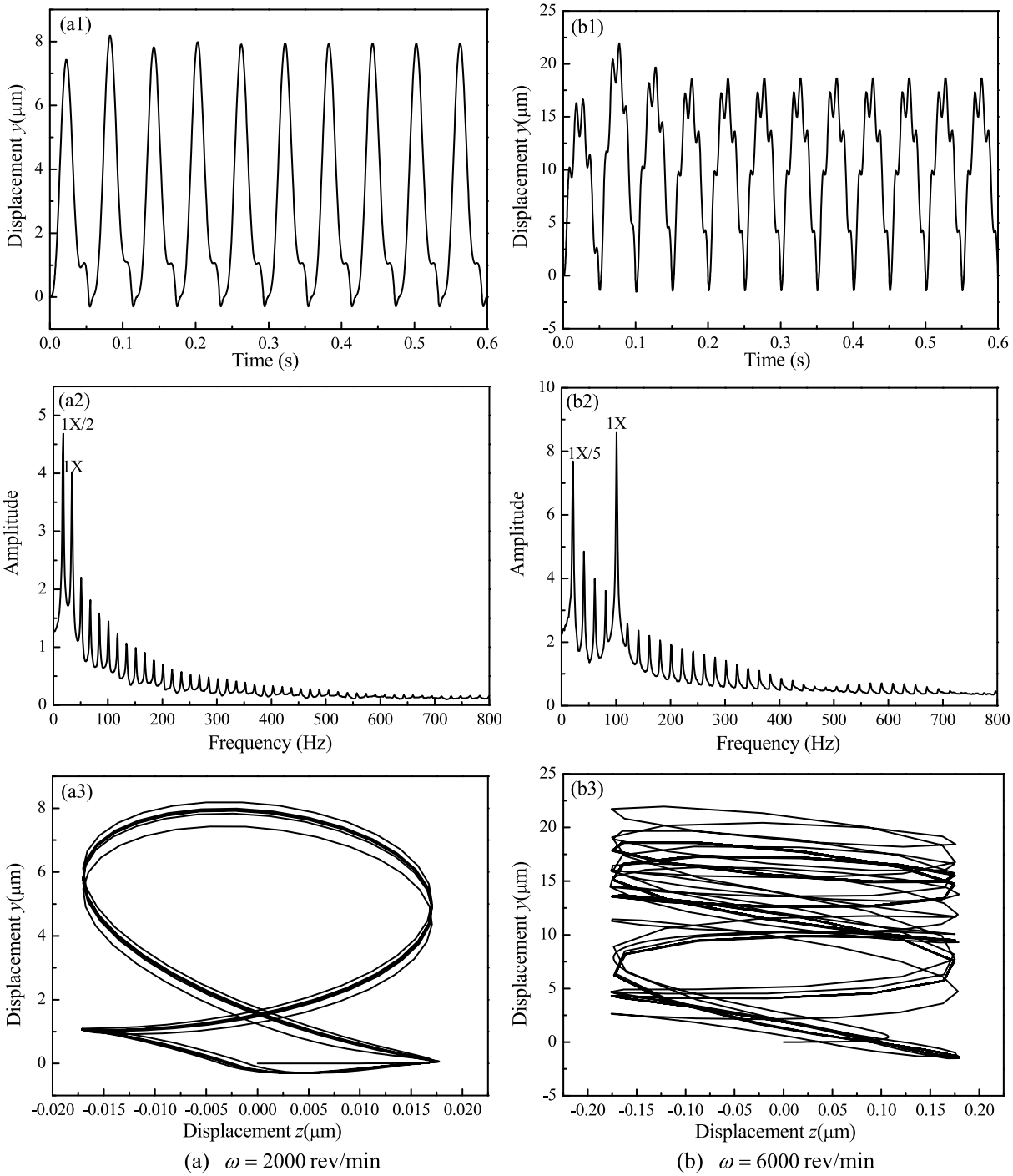

Fig. 7. Vibration characteristics of nodes 6 when $\omega = 2000$ and $\omega = 6000$ rev/min.

3.3. *The effect of foundation stiffness* k_b

Foundation stiffness also influences the vibration of the rotor system. Figure 8 shows the vibration of node 6 with different foundation stiffness when$k_{b1} = 2.2 \times 10^5$ N/m, $\omega = 4000$ rev/min and $\delta_1 = 1$ mm.

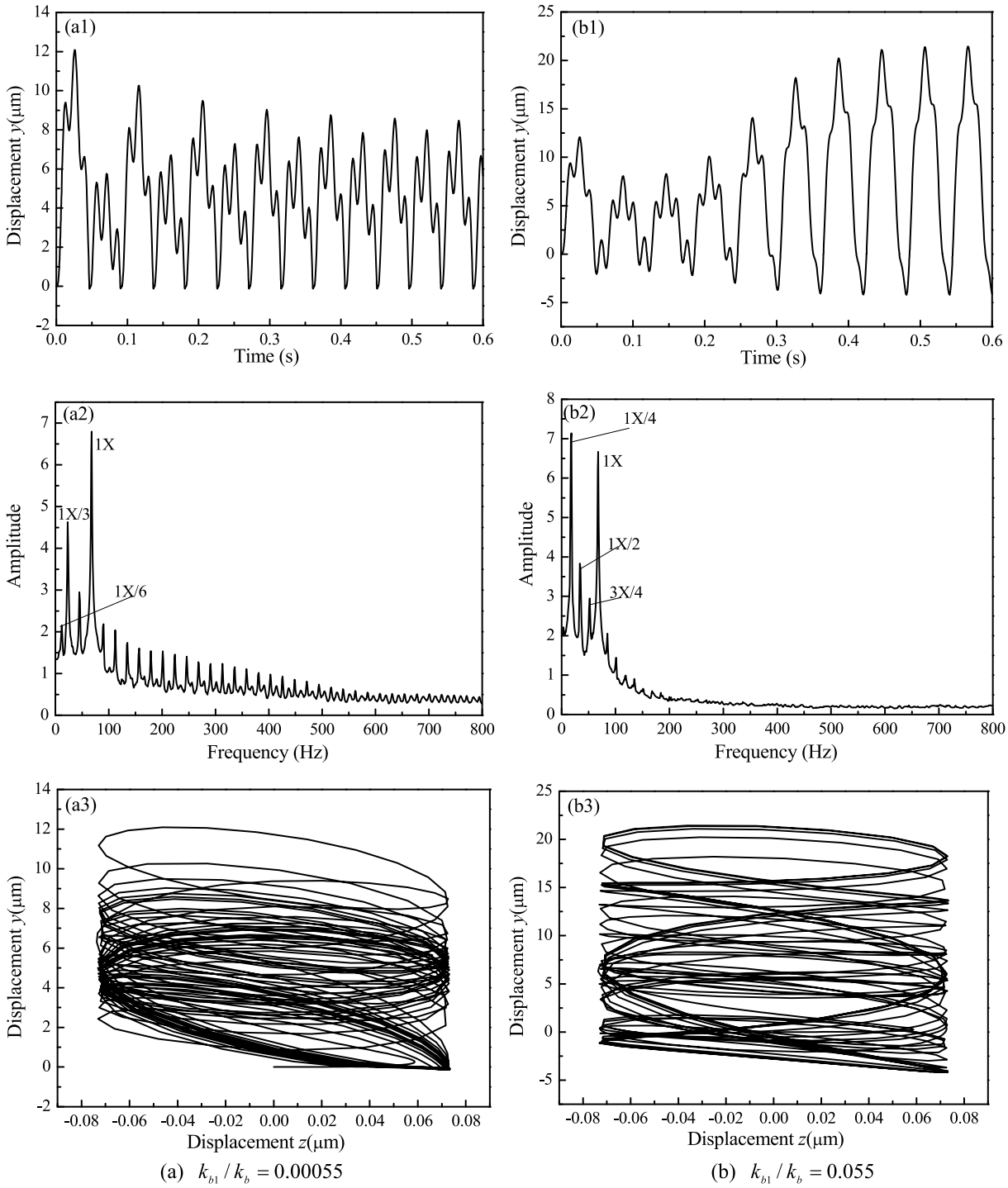

Fig. 8. Vibration characteristics of nodes 6 when $k_{b1}/k_b = 0.00055$ and $k_{b1}/k_b = 0.055$.

From Fig. 8(a), we can see that when $k_{b1}/k_b = 0.00055$, the waveform is similar to that shown in Fig. 6(a), but the amplitude is much smaller. This shows that large foundation stiffness will weaken the vibration of the rotor system. The 1/6 fraction harmonic components such as 1X/6, 2X/6, 3X/6, etc. can be observed in amplitude spectrum. The

Table 4
Response features of pedestal looseness with decrease of k_b

Fixed-parameter	k_{b1}/k_b	Amplitude (peak-peak value μm)	Frequency spectrum characteristics	Motion forms	Rotor trajectory characteristics
$\delta_1 = 1$ mm	0.00055	8.6	The 1/6 fractional harmonic components (1X/6,1X/3,2X/3,etc.)	P-6	Spiral curve
$k_{b1} = 2 \times 10^5$ N/m	0.0055	9.4	The 1/3 fractional harmonic components	P-3	Multiple inside '8' curve
$\omega = 4000$ rev/min	0.055	25.6	The 1/4 fractional harmonic components	P-4	Spiral curve

Table 5
Simulation conditions when $y_b > \delta_1$

Fixed-parameters	variable parameters	Figures
$\omega = 4000$ rev/min, $k_{b1} = 2.2 \times 10^5$ N/m, $k_b = 4 \times 10^6$ N/m	δ_1	Fig. 9
$\omega = 4000$ rev/min, $k_{b1} = 2.2 \times 10^5$ N/m, $k_b = 4 \times 10^8$ N/m	δ_1	Fig. 10

1X/6 component is weak in magnitude and the amplitude of 1X/3 is second only to that of 1X component. So the rotor reaches a period-six motion. Because of the appearance of 1X/6, rotor trajectory is slightly complicated in comparison with that in Fig. 6(a).

Figure 8 (b) shows that the vibration amplitude of node 6 increases greatly until near 0.45s when $k_{b1}/k_b = 0.055$. When the waveform becomes stable, the amplitude is about 25.6 μm, nearly 2.7 times as large as that in Fig. 6(a). The frequency spectrum displays the 1/4 fractional harmonic components such as 1X/4, 1X/2 and 3X/4, etc., which indicates that system motion is period-four, and the amplitude of 1X/4 is largest. The rotor trajectory is still a spiral curve. All these characteristics indicate serious pedestal looseness.

The detailed vibration characteristics of pedestal looseness with decrease of k_b are listed in Table 4. It demonstrates new bifurcation forms with decrease of k_b, large foundation stiffness will weaken the vibration of rotor system, on the contrary, vibration will be exacerbated.

From the foregoing discussion, it is evident that system motion shows basically similar law when stiffness of non-loosened bolts and rotational speed change, and the motion forms are both from period-two through period-three to period-five, which is partly consistent with experiment results (Fig. 5.7.15) in Ref. [2]. But new bifurcation route from period-six through period-three to period-four appears when foundation stiffness decreases, which is similar to experiment results (Fig. 5.7.17) in Ref. [2].

4. Vibration characteristics of rotor system with pedestal looseness when $y_b > \delta_1$

In this section, we investigate the responses of rotor system with pedestal looseness when $y_b > \delta_1$. The pedestal stiffness is given by Eq. (1). Then we study the effect of different parameters on the vibration of the rotor system. These parameters include looseness clearance and foundation stiffness. The simulation conditions are listed in Table 5.

4.1. The effect of looseness clearance under small foundation stiffness condition

The looseness clearance can affect the vibration of the rotor system, Fig. 9 shows the vibration of node 6 with different looseness clearances, $\delta_1 = 8$ μm and $\delta_1 = 7$ μm respectively, when $k_{b1} = 2.2 \times 10^5$ N/m, $k_b = 4 \times 10^6$ N/m and $\omega = 4000$ rev/min.

It can be seen from Fig. 9(a) that when $\delta_1 = 8$ μm, the waveform is truncated in the initial 0.1s and then the waveform turns quickly stable. The maximum displacement is slightly bigger than clearance value, which indicates that pedestal is limited by bilateral constraint when $y_b > \delta_1$. In frequency domain, high order components such as 2X and 3X, etc. can be observed in Fig. 9(a) and the amplitude of 1X is largest. Rotor trajectory is like an inclined long ellipse when system is stable.

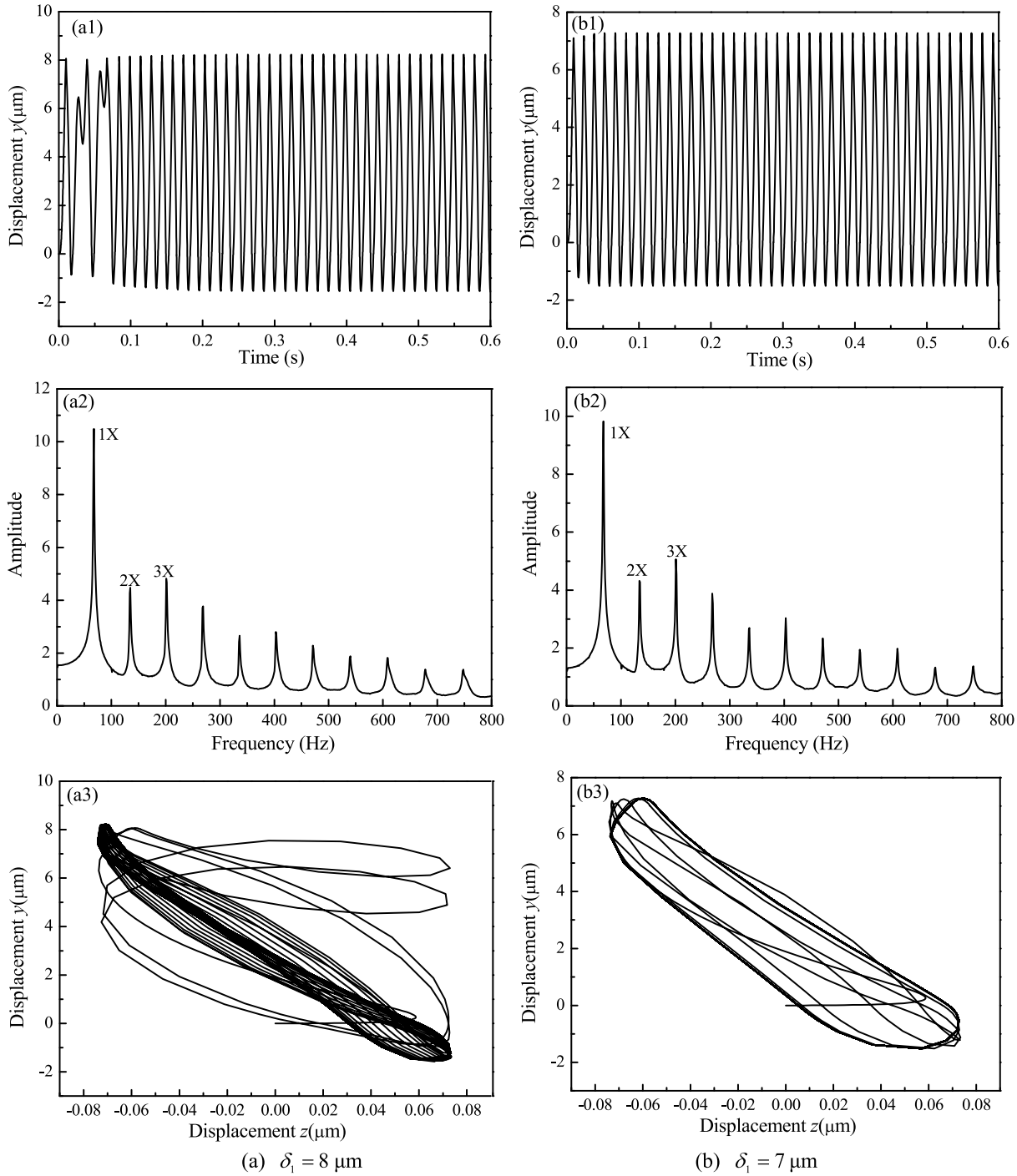

Fig. 9. Vibration characteristics of nodes 6 at $k_b = 4 \times 10^6$ when $\delta_1 = 8$ and $\delta_1 = 7$ μm.

The vibration shown in Fig. 9(b) displays the similar characteristics to that in Fig. 9 (a), but the amplitude of the latter is smaller than that of the former.

The detailed response features of pedestal looseness with decrease of δ_1 are listed in Table 6. From Table 6, it can be seen that system motion always is period-one but vibration amplitude decreases when the value of δ_1 become

Table 6
Response features of pedestal looseness with decrease of δ_1

Fixed parameter	δ_1 (μm)	Amplitude (peak-peak value μm)	Frequency spectrum characteristics	Motion form	Rotor trajectory characteristics
$k_{b1} = 2.2 \times 10^5$ N/m $k_b = 4 \times 10^7$ N/m $\omega = 4000$ rev/min	8	9.8	Multiple harmonic components (1X,2X,3X,etc.)	P-1	An inclined long ellipse
	7	8.8	Multiple harmonic components	P-1	Multiple nested ellipses

Table 7
Vibration characteristics of pedestal looseness with increase of k_b

Fixed-parameter	δ_1 (μm)	Amplitude (peak-peak value μm)	Frequency spectrum characteristics	Motion form	Rotor trajectory characteristics
$k_{b1} = 2.2 \times 10^5$ N/m $k_b = 4 \times 10^8$ N/m $\omega = 4000$ rev/min	8	8.2	Combined frequency	Quasi-period	spiral limited top and bottom in vertical direction
	7	7.2	Continuous spectrum	Quasi-period or chaos	spiral limited top and bottom in vertical direction

smaller. These characteristics indicate that the vibration of the rotor system weakens with the decrease of looseness clearance.

4.2. The effect of looseness clearance under large foundation stiffness condition

The section investigates the effect of looseness clearance on vibration of the rotor system with large foundation stiffness. Figure 10 displays the vibration of node 6 with different looseness clearance, $\delta_1 = 8$ μm and $\delta_1 = 7$ μm respectively, when $k_{b1} = 2.2 \times 10^5$ N/m, $k_b = 4 \times 10^8$ N/m and $\omega = 4000$ rev/min.

From Fig. 10(a), it can be seen that when $\delta_1 = 8$ μm, the waveform is seriously truncated, pedestal collides with constraint, as the concave shown in Fig. 6(b). The increase of constraint stiffness causes the repeated impact and rebound among pedestal, foundation and bolt head. So the displacement is complicated. In frequency domain, combined frequency components (such as 68 Hz + 14 Hz = 82 Hz, 68 Hz + 41 Hz = 109 Hz, etc.) appear in amplitude spectrum, which shows that system motion is quasi-period. The rotor trajectory is similar to spiral limited top and bottom in vertical direction. These features indicate that the system motion is complicated.

When $\delta_1 = 7$ μm, the vibration characteristics of node 6 are shown in Fig. 10(b). Amplitude spectrum is continuous. In such case, the system motion may be quasi-period or chaos. The waveform and rotor trajectory are similar to these in Fig. 10(a) except that the amplitude of the former is less than that of the latter.

The detailed vibration characteristics of pedestal looseness with decrease of δ_1 are listed in Table 7. From Table 7, it can be seen that system motion is quasi-period or chaos, serious truncation of waveform can be observed in waveform, combined frequency components and continuous spectrum appear with decrease of δ_1. These characteristics show that system vibration is more complicated.

From the above discussion, it is clear that system vibration amplitude decreases with the decrease of δ_1. When foundation stiffness is smaller, system motion is period-one. However, when foundation stiffness is larger, system motion is quasi-period or chaos due to the axis moving irregularly.

5. Conclusions

In this study, the pedestal looseness fault is simulated by finite element method. Some results are obtained as follows:

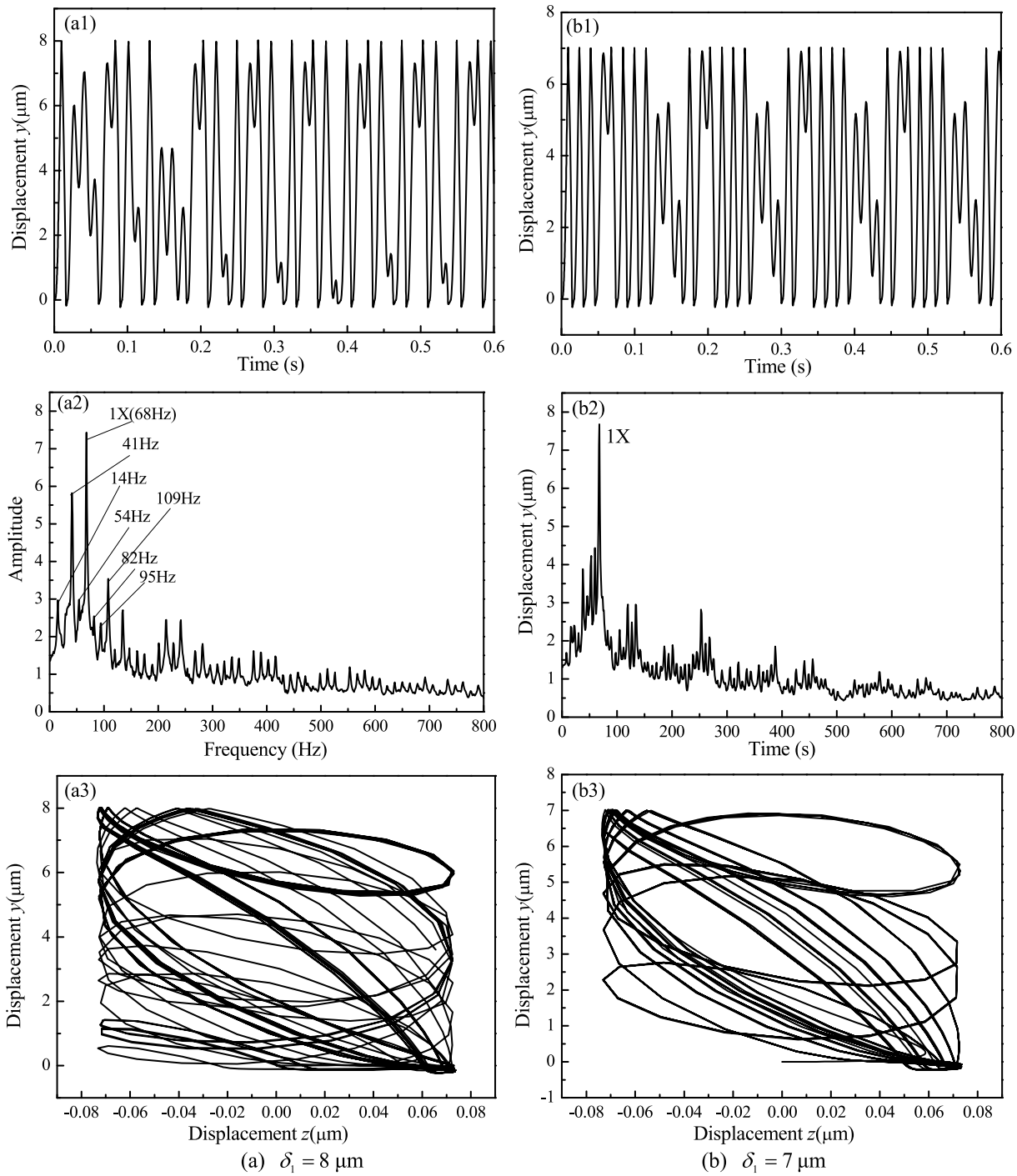

Fig. 10. Vibration characteristics of nodes 6 at $k_b = 4 \times 10^8$ when $\delta_1 = 8$ μm and $\delta_1 = 7$ μm.

(1) When the pedestal displacement of pedestal is less than or equal to the looseness clearance, system motion law is basically the same regardless to the stiffness of non-loosened bolts and rotational speed change. And the motion forms are always from period-two through period-three to period-five. But new bifurcation route from period-six through period-three to period-four will appear when foundation stiffness changes.

(2) When the pedestal displacement of pedestal is greater than the looseness clearance, system vibration amplitude will decrease with the reduction of δ_1. When the stiffness of the foundation is small, the response of the rotor exhibits period-one and high order harmonic components with the decreasing of looseness clearance. However, when the stiffness of the foundation is great, the spectrum of the response of the rotor will be from combined frequency components to the continuous spectrum with the decreasing of the looseness clearance.

Acknowledgments

We are grateful to the China Natural Science Funds (NSFC, Grant No. 50805019) and China's postdoctoral funds (Grant No. 20090450111) for providing financial support for this work.

We would like to express our gratitude to Professor Han and Professor Zhao for revising the paper about English style and grammar, and for offering improving suggestions.

References

[1] B.C. Wen, X.H. Wu, Q. Ding et al., *Theory and Experiment of Nonlinear Dynamics for Rotating Machinery with Faults*, Science Press, Being, 2004, (in Chinese).
[2] A. Muszynska, Rotordynamics, CRC Press, Boca Raton, FL, USA, 2005.
[3] P. Goldman and A. Muszynska, Analytical and experimental simulation of loose pedestal dynamic effects on a rotating machine vibrational response, *Rotating Machinery and Vehicle Dynamics, American Society of Mechanical Engineers* **35** (1991), 11–17.
[4] A. Muszynska and P. Goldman, Chaotic responses of unbalanced rotor bearing stator systems with looseness or rubs, *Chaos, Solitons and Fractals* **5** (1995), 1683–1704.
[5] F. Chu and Y. Tang, Stability and Non-linear responses of a rotor-bearing system with pedestal looseness, *Journal of Sound and Vibration* **241** (2001), 879–893.
[6] W. Lu and F. Chu, Experimental investigation of pedestal looseness in a rotor-bearing system, *Key Engineering Materials* **413–414** (2009), 599–605.
[7] Z. Ji and J.W. Zu, Method of multiple scales for vibration analysis of rotor-shaft systems with non-Linear bearing pedestal model, *Journal of Sound and Vibration* **218**(2) (1998), 293–305.
[8] H. Ma, Z.H. Ren, H.L Yao et al., Numerical simulation and experimental research on pedestal looseness of a rotor system, *ASME 2007 International Design Engineering Technical Conferentces* USA, 2007.
[9] Y. He, Z. Chen, D. Guo and F. Chu, A genetic algorithm based inverse problem approach for pedestal looseness identification in rotor-bearing systems, *Key Engineering Materials* **245–346** (2003), 115–122.
[10] S.M. Lee and Y.S. Choi, Fault diagnosis of partial rub and looseness in rotating machinery using Hilbert-Huang transform, *Journal of Mechanical Science and Technology* **22** (2008), 2151–2162.
[11] C.H. Chen, R.J. Shyu and C.K. Ma, A new fault diagnosis method of rotating machinery, *Shock and Vibration* **15** (2008), 585–598.
[12] C.G. Chien, R.F. Fung and C.L. Tsai, Non-linear vibration analysis of the coupled textile/rotor system by finite element method, *Journal of Sound and Vibration* **221**(1) (1999), 67–84.
[13] J.P. Jing, G. Meng, Y. Sun and S.B. Xia, On the oil-whipping of a rotor-bearing system by a continuum model, *Applied Mathematical Modeling* **29** (2005), 461–475.
[14] Q.K. Han, T. Yu, H. Li, Z.Y. Qin et al., Hybrid model based identification of local rubbing fault in rotor systems, *Key Engineering Materials* **293–294** (2005), 355–364.
[15] D. Guo and Z.K. Peng, Vibration analysis of a cracked rotor using Hilbert–Huang transform, *Mechanical Systems and Signal Processing* **21** (2007), 3030–3041.
[16] Y.Y. He, D. Guo and F.L. Chu, Using genetic algorithms and finite element methods to detect shaft crack for rotor-bearing system, *Mathematics and Computers in Simulation* **57** (2001), 95–108.
[17] M. Behzad and M. Asayeshthe, Numerical and experimental investigation on vibration of rotors with loose discs, *Proceedings of the Institution of Mechanical Engineers, Part C: Journal of Mechanical Engineering Science* **223** (2009), 1–10.
[18] A.S. Lee, B.O. Kim and Y.C. Kim, A finite element transient response analysis method of a rotor-bearing system to base shock excitations using the state-space Newmark scheme and comparisons with experiments, *Journal of Sound and vibration* **297** (2006), 595–615.